Structural Basis for Ligand Selectivity of Heteromeric Olfactory Cyclic Nucleotide-Gated Channels

Mark S. Shapiro* and William N. Zagotta†
*Department of Physiology and Biophysics and †Howard Hughes Medical Institute, University of Washington, Seattle, Washington 98195-7290 USA

ABSTRACT In vertebrate olfactory receptors, cAMP produced by odorants opens cyclic nucleotide-gated (CNG) channels, which allow Ca^{2+} entry and depolarization of the cell. These CNG channels are composed of α subunits and at least two types of β subunits that are required for increased cAMP selectivity. We studied the molecular basis for the altered cAMP selectivity produced by one of the β subunits (CNG5, CNCα4, OCNC2) using cloned rat olfactory CNG channels expressed in *Xenopus* oocytes. Compared with α subunit homomultimers (α channels), channels composed of α and β subunits ($\alpha+\beta$ channels) were half-activated ($K_{1/2}$) by eightfold less cAMP and fivefold less cIMP, but similar concentrations of cGMP. The $K_{1/2}$ values for heteromultimers of the α subunit and a chimeric β subunit with the α subunit cyclic nucleotide-binding region (CNBR) ($\alpha+\beta$-CNBRα channels) were restored to near the values for α channels. Furthermore, a single residue in the CNBR could account for the altered ligand selectivity. Mutation of the methionine residue at position 475 in the β subunit to a glutamic acid as in the α subunit (β-M475E) reverted the $K_{1/2,cAMP}/K_{1/2,cGMP}$ and $K_{1/2,cIMP}/K_{1/2,cGMP}$ ratios of $\alpha+\beta$-M475E channels to be very similar to those of α channels. In addition, comparison of $\alpha+\beta$-CNBRα channels with $\alpha+\beta$-M475E channels suggests that the CNBR of the β subunit contains amino acid differences at positions other than 475 that produce an increase in the apparent affinity for each ligand. Like the wild-type β subunit, the chimeric β/α subunits conferred a shallow slope to the dose-response curves, increased voltage dependence, and caused desensitization. In addition, as for $\alpha+\beta$ channels, block of $\alpha+\beta$CNBRα channels by internal Mg^{2+} was not steeply voltage-dependent ($z\delta \sim 1e^-$) as compared to block of α channels ($z\delta$ 2.7e^-). Thus, the ligand-independent effects localize outside of the CNBR. We propose a molecular model to explain how the β subunit alters ligand selectivity of the heteromeric channels.

INTRODUCTION

The gating of cyclic nucleotide-gated (CNG) channels is the final step in signaling cascades in the sensory neurons of the visual and olfactory systems (Yau and Baylor, 1989; Zufall et al., 1994). These CNG channels are also found in testis, kidney, heart, and brain, where they may provide a mechanism for intracellular cGMP and cAMP to directly modulate the electrical state of the cell and levels of intracellular Ca^{2+} (McCoy et al., 1995; Biel et al., 1994; Weyand et al., 1994; Zufall et al., 1997; Rieke and Schwartz, 1994). Like the kinases, distinct CNG channels are differentially activated by cAMP or cGMP. In the rod photoreceptor, cGMP is the physiological ligand (Tanaka et al., 1989; Baylor and Nunn, 1982), and the CNG channels in the rod strongly select for cGMP over cAMP (Ildefonse et al., 1992; Gordon and Zagotta, 1995b). However, in the olfactory receptor neuron, CNG channels are opened equally well by cAMP, produced by odorant-stimulated activation of adenylyl cyclase (Nakamura and Gold, 1987; Anholt, 1993). Insight into the mechanism of ligand specificity of CNG channels has come from the x-ray structures of catabolite gene-activator protein (CAP) (Weber and Steitz, 1987), a dimeric cAMP-regulated transcription factor, and the regulatory subunit of the cAMP-dependent protein kinase (Su et al., 1995). The cyclic nucleotide-binding region (CNBR) of CNG channels exhibits sequence similarity to that of CAP (Kaupp et al., 1989), and this similarity has given us the opportunity to probe the molecular mechanism of ligand specificity. In CAP, the structure of the CNBR consists of a β-roll, made from eight β strands, followed by two α helices, the B-helix, and the C-helix. The cAMP molecule is bound inside the β-roll, and its purine ring interacts with T127 in the C-helix of the same subunit. Thus, it has been suggested that a region in the putative C-helix in the CNBR of CNG channels plays a pivotal role in determining ligand specificity (Goulding et al., 1994; Varnum et al., 1995). In particular, Varnum et al. (1995) showed that D604 in the rod CNG channel α subunit, at a position equivalent to T127 in CAP, is responsible for the high specificity for cGMP over cAMP in these channels. Mutation of D604 to methionine caused a dramatic decrease in the efficacy of cGMP, and an increase in the efficacy of cAMP, as agonists (Varnum et al., 1995; Sunderman and Zagotta, 1999a).

The cloning of the rod (Kaupp et al., 1989) and olfactory (Dhallan et al., 1990; Ludwig et al., 1990) CNG channel α subunits has demonstrated that these channels are members of the voltage-activated family of channels (Jan and Jan, 1990, 1992). Like voltage-activated channels, CNG channels contain six membrane-spanning segments, a pore-forming P-region, and a tetrameric arrangement of subunits (see Zagotta and Siegelbaum, 1996 for a review). Native

Received for publication 26 October 1999 and in final form 9 February 2000.

Address reprint requests to William N. Zagotta, Ph.D., Dept. of Physiology and Biophysics, HHMI Box 357370, University of Washington, Seattle, WA 98195-7290. Tel.: 206-685-3878; Fax: 206-543-0934; E-mail: zagotta@u.washington.edu.

0006-3495/00/05/2307/14 $2.00

CNG channels are heteromultimers of at least two kinds of subunits, α and β. When expressed alone, olfactory α (CNG2, CNCα3, OCNC1) subunits produce functional homomeric channels, whereas β subunits alone do not produce CNG currents (Chen et al., 1993; Bradley et al., 1994; Liman and Buck, 1994; Korschen et al., 1995; Sautter et al., 1998; Bonigk et al., 1999). Recently, it has been shown that the native olfactory channel contains two types of β subunits. Heteromeric channels containing both types of β subunits behave more like native olfactory channels than do channels containing only one type of β subunit (Sautter et al., 1998; Finn et al., 1998; Bonigk et al., 1999). One type of β subunit (CNG4.3, CNCβ1b) is an alternatively spliced variant of the rod β subunit and was recently cloned from olfactory epithelium (Sautter et al., 1998; Bonigk et al., 1999). The other type of β subunit (CNG5, CNCα4, OCNC2) is expressed at high levels in sensory neurons of the primary olfactory epithelium and vomeronasal organ (Liman and Buck, 1994; Bradley et al., 1994; Berghard et al., 1996) and will be referred to in this study as the olfactory β subunit. This subunit has 52% sequence identity with the olfactory α subunit, and 30% sequence identity with the rod β subunit (Bradley et al., 1994; Liman and Buck, 1994). It has a membrane topology similar to the α subunit but lacks much of the amino-terminal region of the olfactory α subunit. This region of the olfactory α subunit has been shown to be an autoexcitatory/calmodulin binding domain that strongly interacts with the gating machinery of the CNBR (Liu et al., 1994; Varnum and Zagotta, 1997).

Incorporation of the olfactory β subunit changes the gating properties of the olfactory channels. Channels composed of both α and β subunits ($\alpha+\beta$ channels) are half-activated ($K_{1/2}$) by much lower concentrations of cAMP than channels composed of only α subunits (α channels) (Liman and Buck, 1994; Bradley et al., 1994). Since cAMP is the ligand for these channels in olfactory neurons, this raises the possibility that the role of β subunits is precisely to achieve the necessary high apparent affinity of cAMP, making the functional effect of the β subunit of particular physiological significance. In this study we focus on the olfactory β subunit and investigate how this β subunit affects CNG channel gating and pharmacology, and explored the structural determinants of these effects. By comparing the properties of α channels, $\alpha+\beta$ channels, and $\alpha+$chimeric β/α channels, we show that the effects of the β subunit on ligand specificity localize to the CNBR, while the effects on the slope of the dose-response relation, voltage dependence, desensitization, and Mg^{2+} block localize outside the CNBR. Furthermore, we show that a single residue in the C-helix of the CNBR could account for the altered ligand specificity.

METHODS

The cDNA for the α subunit (CNG2, CNCα3, OCNC1) and the β subunit (CNG5, CNCα4, OCNC2) of the rat olfactory CNG channel were kindly provided by the laboratories of R. R. Reed (The Johns Hopkins School of Medicine, Baltimore, MD) and Kai Zinn (California Institute of Technology, Pasadena, CA), respectively. These cDNAs were separately subcloned into a high expression vector, kindly provided by E. R. Liman, that contains the untranslated sequences of the *Xenopus* β-globin gene (Liman et al., 1992). In general, the oocyte expression and electrophysiology were like those previously described (Gordon and Zagotta, 1995a). Briefly, *Xenopus* oocytes were injected with in vitro transcribed RNA coding for channel subunits, incubated for 3–7 days at 16°C, and then patch-clamped in the inside-out configuration. Intracellular and extracellular solutions contained 130 mM NaCl, 0.2 mM EDTA, and 3 mM HEPES, pH 7.2. For some experiments, niflumic acid (500 μM final concentration) was added to the pipette (extracellular) solution to reduce endogenous Ca^{2+}-activated Cl^- currents. Cyclic nucleotides were added to the internal solution at the concentrations indicated. The cDNAs for the chimeric subunits were generated using a method based on PCR like that previously described (Gordon and Zagotta, 1995a) and were verified by sequence analysis. For the β-CNBRα chimera, the sequence between C352 and E491 of the β subunit was replaced by the sequence between C460 and S593 of the α subunit. The β-C5α chimera had the following mutations in the β subunit: M464L, K467R, L473M, M475E, N476G.

We generated heteromeric channels by co-injecting RNA for the α subunit together with either the wild-type β subunit or a chimeric β/α subunit. We found that co-injecting RNA for the subunits at a ratio of 4:1 α:β maximized expression of heteromultimers. The experiments summarized in Fig. 6, showing the results from a range of α:β RNA injection ratios from 2:1 to 100:1, indicate that an injection ratio of 4:1 produces sufficient β subunits to form almost exclusively heteromeric channels of their preferred subunit composition (Shapiro and Zagotta, 1998). Thus, all the rest of the data from heteromultimers were from RNA injection ratios of ~4:1. Heteromeric channels have a 1:1 stoichiometry (Shapiro and Zagotta, 1998), and so we interpret the optimal 4:1 injection ratio as reflecting a greater translational efficiency of β versus α subunits. Due to the large effect of the β subunit on the apparent affinity of the channel for cAMP, a population of α-homomultimers in the coinjection experiments >10% would be easily seen in the dose-response curve. We did not see evidence of α-homomultimers with an injection ratio of 4:1.

For patches with homomeric α channels, voltage pulses were applied every 3–5 s. Currents from heteromeric $\alpha+\beta$ or $\alpha+$chimeric β/α channels desensitized. For these channels, cyclic nucleotide-free solution was perfused for a minimum of 20 s before each application of ligand, and voltage pulses to these patches were applied every 1 s. Once ligand was applied, the pulse with the greatest current was used for the measurement. Using this protocol, we estimate that errors from desensitization were seldom greater than 15% for any given measurement.

For the Mg^{2+} experiments (Fig. 7), we added to our usual internal solution various amounts of $MgCl_2$ to obtain solutions with various free [Mg^{2+}], calculated using the MAXC program written by Chris Patton, Stanford University. For solutions containing a free [Mg^{2+}] of 120 μM, 811 μM, 2.81 mM, 9.81 mM, and 29.8 mM, the amount of $MgCl_2$ added was 300 μM, 1 mM, 3 mM, 10 mM, and 30 mM, respectively.

RESULTS

We studied cloned rat olfactory CNG channels expressed in *Xenopus* oocytes using the inside-out configuration of the patch-clamp technique. Oocytes injected solely with RNA coding for the olfactory α subunit produced homomeric channels (α channels). Fig. 1 shows currents from α channels in response to various concentrations of cAMP, cGMP, or cIMP. Currents were recorded using successive pulses to −60 and 60 mV from a holding potential of 0 mV (Fig. 1, *inset*). To elicit CNG current, cyclic nucleotides were ap-

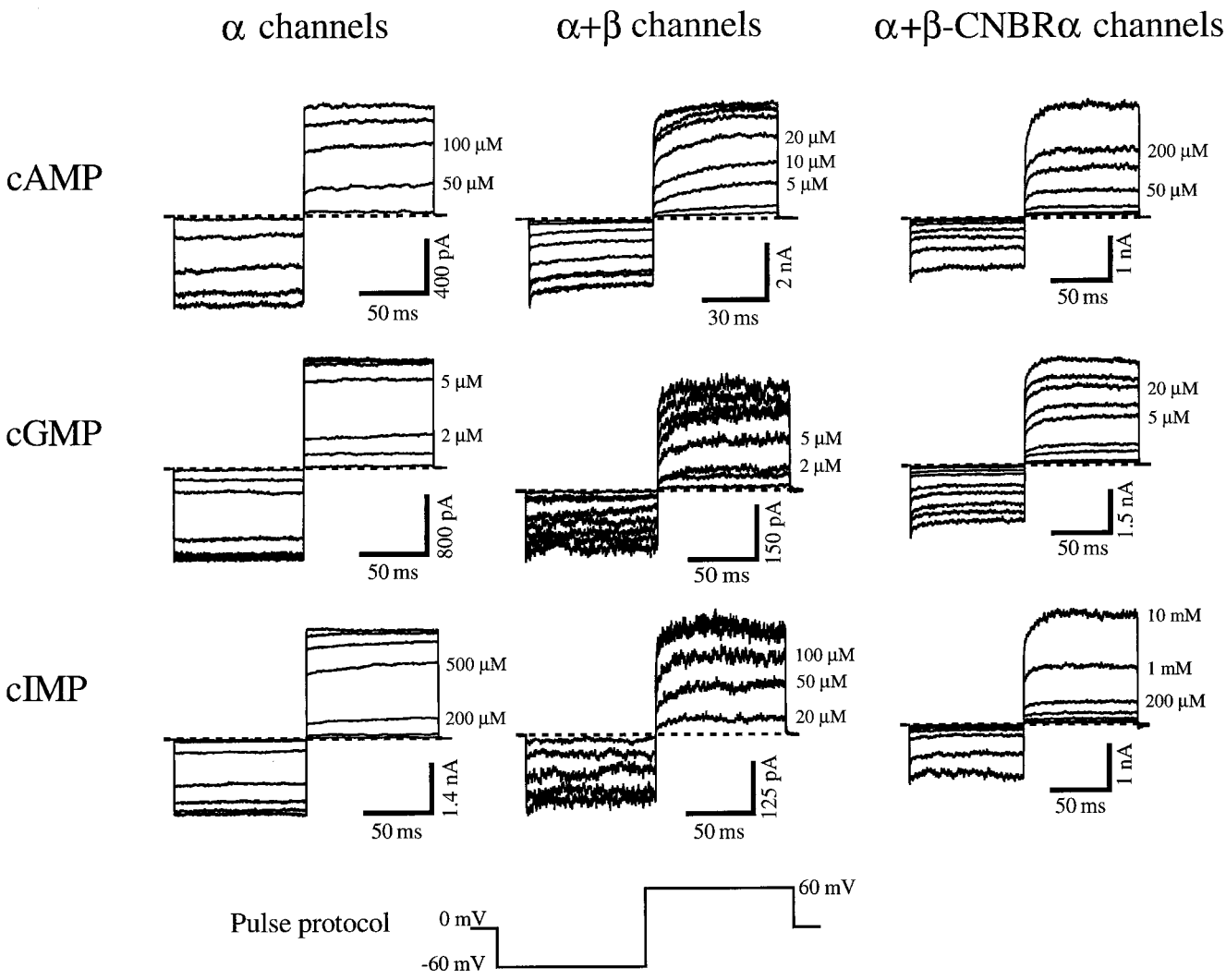

FIGURE 1 Currents in homomeric α channels, heteromeric α+β channels, and heteromeric α+β-CNBRα channels activated by a range of concentrations of cAMP, cGMP, and cIMP. The pulse protocol used is shown at the bottom. Selected concentrations near half-maximal activation are labeled. For α channels, the cAMP concentrations were (μM) 10, 20, 50, 100, 200, 1000; the cGMP concentrations were (μM) 0.5, 1, 2, 5, 10, 20, 50, 100; and the cIMP concentrations were 50 μM, 100 μM, 200 μM, 500 μM, 1 mM, 2 mM, 10 mM. For α+β channels, the cAMP concentrations were (μM) 1, 2, 5, 10, 20, 50, 100, 200, 1000; the cGMP concentrations were (μM) 0.5, 1, 2, 5, 10, 20, 50, 100; and the cIMP concentrations were (μM) 10, 20, 50, 100, 200, 1000. For α+β-CNBRα channels, the cAMP concentrations were (μM) 5, 10, 20, 50, 100, 200, 1000; the cGMP concentrations were (μM) 0.2, 0.5, 1, 2, 5, 10, 20, 50, 100; and the cIMP concentrations were 10 μM, 20 μM, 50 μM, 100 μM, 200 μM, 1 mM, 10 mM. For α channels, currents are from three different patches. For α+β channels, the currents in cGMP and cIMP are from the same patch, and the currents in cAMP are from a different patch. For α+β-CNBRα channels, currents in cAMP and cGMP are from the same patch, and the currents in cIMP are from a different patch.

plied to the intracellular side of the patch and the leak currents in the absence of cyclic nucleotide were subtracted. For cAMP and cGMP, the properties of these α channels were very similar to those previously described for homomeric channels of the olfactory α subunit (Dhallan et al., 1990).

Oocytes injected only with RNA for the β subunit (CNG5, CNCα4, OCNC2) did not express functional CNG channels. However, oocytes co-injected with RNA coding for both the α subunit and the β subunit expressed heteromeric channels formed from both the α and β subunits (α+β channels) with gating and pharmacological properties different from α channels (Liman and Buck, 1994; Bradley et al., 1994). Compared to α channels, α+β channels were activated by much lower concentrations of cAMP and cIMP, but similar concentrations of cGMP. In addition, the currents exhibited a slow relaxation to steady state after a voltage step. This may reflect greater voltage dependence or slower gating of the heteromeric channels, such that more channels are open at depolarized versus hyperpolarized potentials. These currents also exhibited greater rectification at saturating concentrations of ligand than the currents from α channels. Finally, α+β channels, but not α channels, expressed in oocytes desensitized after the application of

ligand over a period of several seconds (Fig. 2). Thus, when recording from heteromultimers, every application of ligand was preceded by >20 s in cyclic nucleotide-free control solution, which was sufficient time for full recovery (data not shown). Collectively, these identifying characteristics clearly distinguish between channels composed of α subunits and those composed of both α and β subunits, and represent the signature effects of the β subunit.

To localize the region of the β subunit responsible for the altered properties, we first constructed a chimeric β subunit with the α subunit cyclic nucleotide-binding region (β-CNBRα). Like the wild-type β subunit, the chimeric subunit did not yield functional CNG channels when expressed alone, but when co-expressed with the α subunit yielded heteromeric channels ($\alpha+\beta$-CNBRα channels) with some properties like α channels and some properties like $\alpha+\beta$ channels. Like $\alpha+\beta$ channels, $\alpha+\beta$-CNBRα channels also exhibited a slow relaxation to steady state after a voltage step and rectification at saturating concentrations of cyclic nucleotides (Fig. 1). In addition, they also desensitized like $\alpha+\beta$ channels (Fig. 2). However, $\alpha+\beta$-CNBRα channels are activated by concentrations of cAMP, cGMP, and cIMP similar to α channels. We also generated the inverse chimera, consisting of the α subunit with the CNBR of the β subunit, but that chimera did not produce functional channels, either alone or as a heteromultimer with the α subunit.

Dose-response curves for activation of channels by cAMP, cGMP, and cIMP from patches expressing α channels, $\alpha+\beta$ channels, or $\alpha+\beta$-CNBRα channels are shown in Fig. 3. There were two robust effects of co-expression of the wild-type β subunit on the dose-response relation: a marked ligand-specific increase in the apparent affinity of the channel for cAMP and cIMP, and a ligand-nonspecific decrease in the slope of the dose-response curve. We quantified CNG channel gating by fitting dose-response data with the Hill equation. For cAMP (Fig. 3 *A*), the concentration that gave half-maximal current ($K_{1/2}$) at 60 mV in patches with α channels was 83 $\pm$ 3 μM (mean $\pm$ SEM, $n = 26$), but about eightfold less, 10.1 $\pm$ 0.7 μM ($n = 22$) for patches with $\alpha+\beta$ channels. For cGMP, however (Fig. 3 *B*), $K_{1/2}$ was similar for the two channel types: 2.8 $\pm$ 0.1 μM ($n = 10$) for α channels and 4.8 $\pm$ 0.8 μM ($n = 6$) for $\alpha+\beta$ channels. These results for activation of $\alpha+\beta$ channels by cAMP and cGMP are very similar to those reported (Liman and Buck, 1994; Bradley et al., 1994). As for cAMP, the presence of the β subunit had a large effect on the apparent affinity of the channel for cIMP (Fig. 3 *C*). For α channels, $K_{1/2}$ was 350 $\pm$ 34 μM ($n = 10$), but for $\alpha+\beta$ channels, $K_{1/2}$ was 86 $\pm$ 21 μM ($n = 3$). For all three ligands, the slope of the dose-response curve was considerably less for $\alpha+\beta$ channels (Hill coefficients = 1.3–1.5) than for α channels (Hill coefficients = 2.1–2.6).

Dose-response relations for $\alpha+\beta$-CNBRα channels indicated that their specificity for the three ligands reverted to be like α channels (Fig. 3). Data for activation of channels by cAMP, cGMP, and cIMP were fit by Hill equations with $K_{1/2}$ values of 119 $\pm$ 9 μM ($n = 9$), 7.0 $\pm$ 0.5 μM ($n = 8$), and 598 $\pm$ 152 μM ($n = 3$), respectively. However, Hill coefficients for activation of $\alpha+\beta$-CNBRα channels by the three ligands (1.1–1.4) were similar to those for activation of $\alpha+\beta$ channels. Thus, substitution of the α subunit CNBR into the β subunit nearly restores the $K_{1/2}$ values to be like α homomultimers; however, the shallow slopes of the dose-response curves remain. We conclude that the ligand-specific shift of the apparent affinities caused by the β subunit localizes to the CNBR, but the ligand-nonspecific shallowing of the dose-response relation, slow gating, rectification, and desensitization localize to a different part of the protein.

Structural basis for ligand specificity in the CNBR

To further localize the structural basis for the alterations in ligand specificity produced by the β-CNBRα chimera, we made more restricted chimeras within this domain. We focused on amino acid differences that were predicted from the CAP structure to be within 5–10 Å from the purine ring, the portion of the cyclic nucleotide that differs between cAMP, cGMP, and cIMP. A cluster of such residues was found in the putative C-helix of the CNBR, and we replaced five residues in the C-helix of the β subunit (M464L, K467R, L473M, M475E, N476G) with the corresponding residues of the α subunit (β-C5α). Replacement of these five residues dramatically increased the apparent affinity for

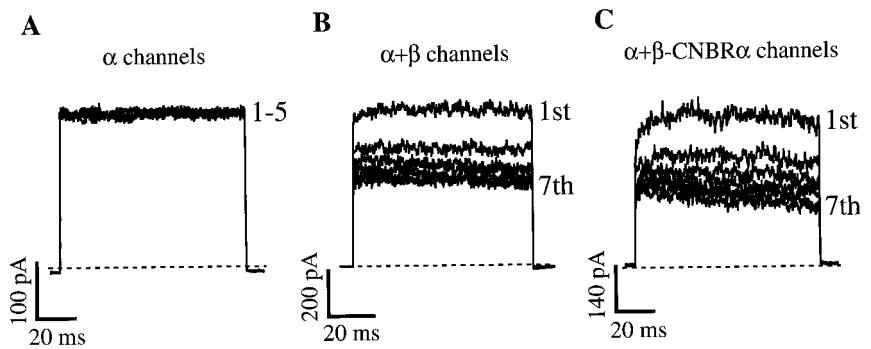

FIGURE 2 Desensitization. Currents from patches containing homomeric α channels (*A*), heteromeric $\alpha+\beta$ channels (*B*), or heteromeric $\alpha+\beta$-CNBRα channels (*C*), activated by 1 mM cAMP. Patches were held at 0 mV, and voltage pulses were applied to 60 mV every 1 s. In each case, the first pulse shown was given within 1 s of application of ligand. In *A–C*, the first five, seven, and seven pulses are shown, respectively.

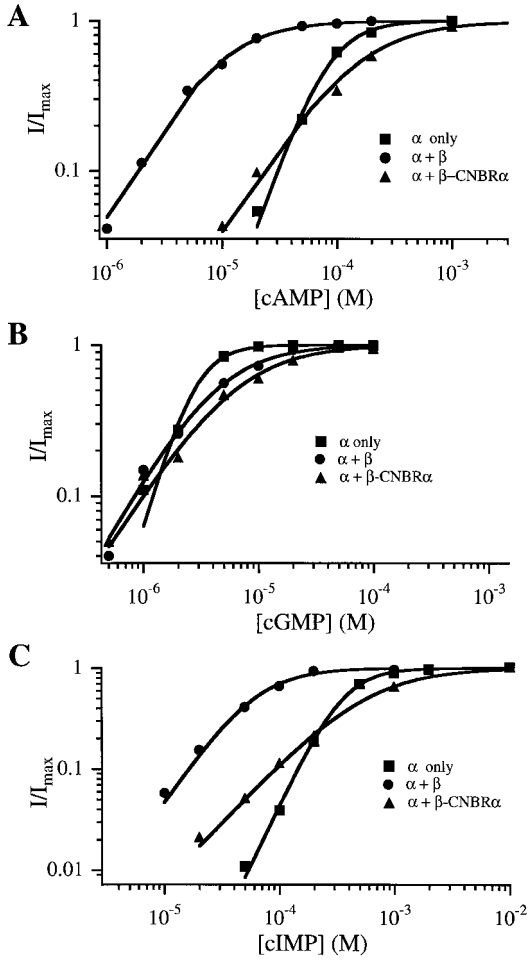

FIGURE 3 Dose-response data. Data are the amplitude of CNG currents at 60 mV elicited by a range of cyclic nucleotide concentrations, normalized to the maximum current, for α channels (*squares*), $\alpha+\beta$ channels (*circles*), or $\alpha+\beta$-CNBRα channels (*triangles*) for cAMP (*top*), cGMP (*middle*), and cIMP (*bottom*). Superimposed on the data are fits to Hill equations of the form $I = I_{max}([cNMP]^n/K^n_{1/2} + [cNMP]^n)$, where [cNMP] is the concentration of ligand, $K_{1/2}$ is the concentration that produces half-maximal current, and n is the Hill coefficient. For activation of α channels by cAMP, cGMP, and cIMP, $K_{1/2}$ = 85 μM, 2.8 μM, 363 μM and n = 2.2, 2.7, 2.4, respectively. For activation of $\alpha+\beta$ channels by cAMP, cGMP, and cIMP, $K_{1/2}$ = 8.8 μM, 4.3 μM, 61 μM and n = 1.4, 1.3, 1.7, respectively. For activation of $\alpha+\beta$-CNBRα channels by cAMP, cGMP, and cIMP, $K_{1/2}$ = 143 μM, 6.3 μM, 579 μM and n = 1.2, 1.2, 1.2, respectively.

cGMP and decreased the apparent affinity for cAMP of $\alpha+\beta$-C5α channels compared to $\alpha+\beta$ channels (Fig. 4, *A* and *B*). For activation of $\alpha+\beta$ channels by cGMP, $K_{1/2}$ was 4.8 ± 0.8 μM (n = 6), but for $\alpha+\beta$-C5α channels, $K_{1/2}$ decreased by >10-fold to 0.34 ± 0.03 μM (n = 5). The $K_{1/2}$ for activation of $\alpha+\beta$-C5α channels by cAMP, however, was actually increased by almost twofold from 10.1 ± 0.7 μM (n = 22) for $\alpha+\beta$ channels to 18.5 ± 1.9 μM (n = 7) for $\alpha+\beta$-C5α channels.

One of the mutations made in the β-C5α chimera was M475E. This residue is at a position equivalent to D604 in the rod α subunit that has previously been shown, for rod α channels, to have a dramatic effect on cyclic-nucleotide specificity (Varnum et al., 1995). To test whether a difference at this residue alone might be able to account for the effects of the β subunit on cyclic nucleotide specificity, we constructed the point mutation M475E in the β subunit. Co-expression of this β-M475E subunit with olfactory α subunits also yielded channels with a greatly increased apparent affinity for cGMP, and decreased apparent affinity for cAMP (Fig. 4 *C*). For activation of these $\alpha+\beta$-M475E channels by cGMP and cAMP, $K_{1/2}$ was 0.55 ± 0.05 μM (n = 4) and 37 μM ± 4 μM (n = 4), respectively. Thus, the β-M475E mutation produces large, ligand-specific alterations in the apparent affinities of the olfactory heteromeric channels, similar to those seen in rod α channels (Varnum et al., 1995; Varnum and Zagotta, 1996). In addition, comparison of $\alpha+\beta$-CNBRα channels with $\alpha+\beta$-M475E channels suggests that the CNBR of the β subunit contains amino acid differences at positions other than 475 that produce an increase in the apparent affinity for each ligand.

We calculated the ratio of $K_{1/2}$ values for cAMP and cGMP ($K_{1/2,cAMP}/K_{1/2,cGMP}$) as a measure of the cAMP-to-cGMP selectivity (Fig. 4 *D*). For olfactory α-homomultimers, cGMP is a more potent agonist than cAMP; $K_{1/2,cAMP}/K_{1/2,cGMP}$ for these channels is nearly 30. The effect of the β subunit in the channel is to greatly increase the apparent affinity of cAMP relative to cGMP, decreasing $K_{1/2,cAMP}/K_{1/2,cGMP}$ to ~2. Replacing the CNBR of the β subunit with that of the α subunit almost completely reversed this effect, so that $K_{1/2,cAMP}/K_{1/2,cGMP}$ for $\alpha+\beta$-CNBRα channels was more similar to that for α channels. Furthermore, replacing just the C-helix (β-C5α) or only a single residue within the C-helix (β-M475E) was sufficient to produce high cGMP-to-cAMP specificity. We conclude that the residue at position 475 in the olfactory β subunit plays a significant role in ligand discrimination, and that, like in rod α subunits, an acidic amino acid at this position induces high cGMP-to-cAMP selectivity. A methionine residue at this position in the olfactory β subunit allows for activation of the heteromultimeric olfactory channels by cAMP, its physiological ligand.

The residue at position 475 in the β subunit also plays a key role in determining the cIMP-to-cGMP specificity in olfactory heteromeric channels. Both $\alpha+\beta$-C5α channels and $\alpha+\beta$-M475E channels exhibited an apparent affinity for cIMP only slightly higher than the apparent affinity of cIMP for $\alpha+\beta$ channels (Fig. 5, *A–C*). For $\alpha+\beta$-C5α channels, the $K_{1/2}$ for activation by cIMP was 37 ± 9 μM (n = 3), and for $\alpha+\beta$-M475E channels, the $K_{1/2}$ was 53 ± 7 μM (n = 4). However, the $K_{1/2,cIMP}/K_{1/2,cGMP}$ ratios for these channels were much more similar to those of the α channels than to those of $\alpha+\beta$ channels (Fig. 5 *D*). This result reflects the fact that the β-C5α chimera and β-M475E point mutation are having a much larger effect on activation by cGMP than on activation by cIMP. Since cGMP and

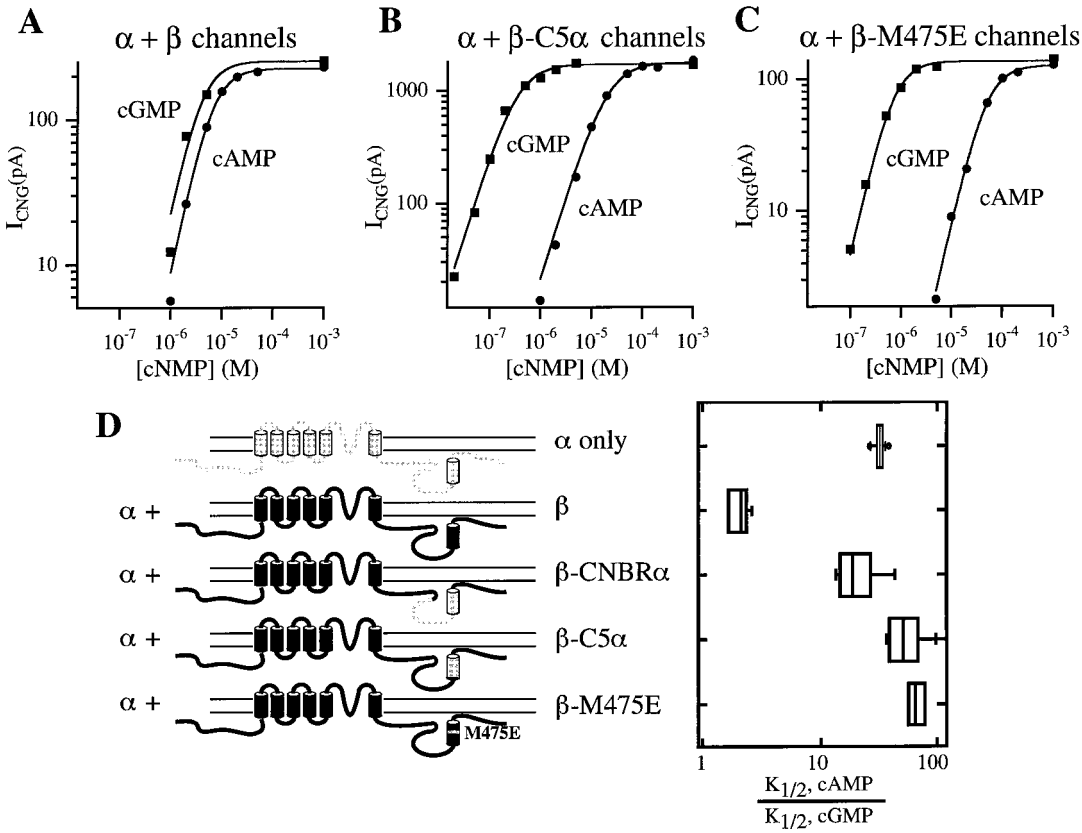

FIGURE 4 Effect of chimeras in the C-helix on cAMP selectivity. Data are the amplitude of CNG currents at 60 mV elicited by a range of concentrations of cAMP and cGMP for $\alpha+\beta$ channels (*A*), $\alpha+\beta$C5α channels (*B*), or $\alpha+\beta$-M475E channels (*C*). Superimposed on the data are fits to Hill equations, as described in the legend to Fig. 3. For activation of $\alpha+\beta$ channels by cAMP and cGMP, $K_{1/2}$ = 6.38 μM and 3.85 μM and n = 1.7 and 1.7, respectively. For activation of $\alpha+\beta$C5α channels by cAMP and cGMP, $K_{1/2}$ = 20 μM and 0.34 μM and n = 1.5 and 1.5, respectively. For activation of $\alpha+\beta$-M475E channels by cAMP and cGMP, $K_{1/2}$ = 48 μM and 0.69 μM and n = 1.7 and 1.7, respectively. Plotted in *D* are box plots for the ratio of $K_{1/2}$ values for cAMP to cGMP for these three channels. The vertical line in the middle of each box marks the median of the data. The box shows the middle half of the data, between the 25th and 75th percentiles. The "whiskers" show the data between the 5th and 95th percentiles. The circles are the extreme points in the data.

cIMP differ at only the 2 position of the purine ring, this result suggests that, like in the α subunit, the amino acid at 475 is able to interact with this region of the cyclic nucleotide molecule.

For α and $\alpha+\beta$ channels, all three cyclic nucleotides activated the same maximal current. For α channels, the ratio of the current activated by saturating concentrations of cAMP to that activated by saturating concentrations of cGMP ($I_{cAMP,\ sat}/I_{cGMP,\ sat}$) was near one (Table 1). The ability of these ligands to activate the same maximal current in α channels arises from the energetically favorable opening transition of this channel (Gordon and Zagotta, 1995b). For $\alpha+\beta$ channels, $I_{cAMP,\ sat}/I_{cGMP,\ sat}$ was also near one. That these ligands can activate the same maximal current for $\alpha+\beta$ channels as well suggests, but does not prove, that opening is energetically favorable for $\alpha+\beta$ channels also (Table 1). In theory, the increased time-dependence and rectification of $\alpha+\beta$ channels versus α channels could reflect a less favorable opening transition in $\alpha+\beta$ channels. However, currents from three heteromeric channels with different cyclic nucleotide selectivities ($\alpha+\beta$ channels, $\alpha+\beta$-M475E channels, and $\alpha+\beta$-C5α channels) all displayed time-dependent rectification and $I_{cAMP,\ sat}/I_{cGMP,\ sat}$ values near one at both −60 mV and +60 mV (data not shown). This suggests either the unlikely possibility that the opening transition is unfavorable and cyclic nucleotide-independent in these heteromeric channels, or more likely, that the opening transition is favorable and the time-dependent rectification comes from additional closed states apart from those leading to opening. Voltage-dependent occupancy of these additional closed states could produce a greater voltage dependence in maximal open probability, such that fully liganded heteromeric channels spend more time open at 60 mV than at −60 mV. Comparison of currents obtained by stepping patches held at 0 mV directly to 60 mV or −60 mV suggests that both this mechanism and open-channel rectification may contribute to increased steady-state rectification. Using this protocol, the instanta-

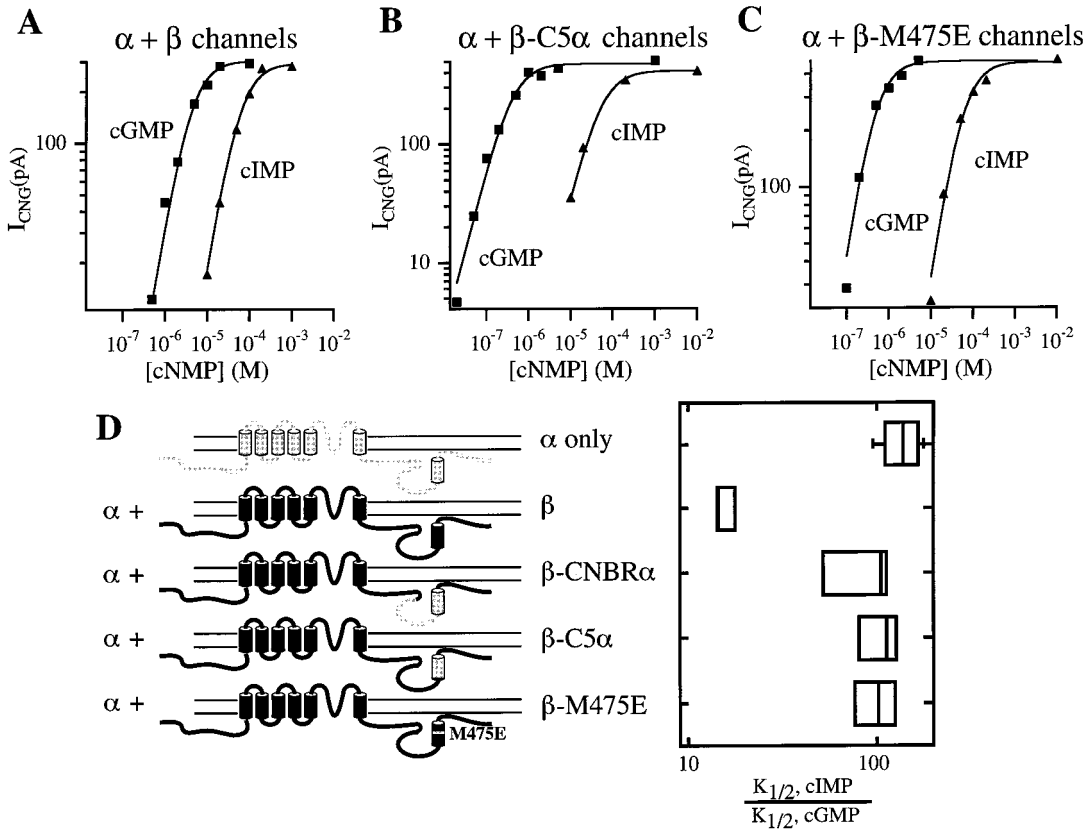

FIGURE 5 Effect of chimeras in the C-helix on cIMP selectivity. Data are the amplitude of CNG currents at 60 mV elicited by a range of concentrations of cGMP and cIMP, for $\alpha+\beta$ channels (*A*), $\alpha+\beta$C5α channels (*B*), or $\alpha+\beta$-M475E channels (*C*). Superimposed on the data are fits to Hill equations, as described in the legend to Fig. 3. For activation of $\alpha+\beta$ channels by cGMP and cIMP, $K_{1/2}$ = 4.3 μM and 61 μM and n = 1.5 and 1.5, respectively. For activation of $\alpha+\beta$C5α channels by cGMP and cIMP, $K_{1/2}$ = 0.41 μM and 55 μM and n = 1.4 and 1.4, respectively. For activation of $\alpha+\beta$-M475E channels by cGMP and cIMP, $K_{1/2}$ = 0.46 μM and 55 μM and n = 1.5 and 1.5, respectively. Plotted in *D* are box plots for the ratio of $K_{1/2}$ values for cIMP to cGMP for these three channels. The vertical line in the middle of each box marks the median of the data. The box shows the middle half of the data, between the 25th and 75th percentiles. The "whiskers" show the data between the 5th and 95th percentiles.

neous current at the start of the voltage step, which should reflect open-channel properties, was greater at 60 mV than at −60 mV (data not shown).

For $\alpha+\beta$-CNBRα channels, saturating concentrations of cAMP produced only ~75% of the current produced by saturating concentrations of cGMP. This smaller current

TABLE 1 Parameters for activation of channels by cAMP

Channel	$K_{1/2}$, cAMP, 60 mV (μM)	$K_{1/2}$, cAMP, −60 mV (μM)	"n," cAMP, 60 mV	I_{-60}/I_{60}, cAMP (maximal)	I_{cAMP}/I_{cGMP} (maximal, 60 mV)
α channels	83 ± 3	89 ± 3	2.33 ± 0.06	0.79 ± 0.01	0.98 ± 0.02
	n = 26	n = 26	n = 25	n = 28	n = 12
$\alpha+\beta$ channels	10.1 ± 0.7	16.3 ± 1.0	1.49 ± 0.04	0.52 ± 0.01	1.11 ± 0.03
	n = 22	n = 22	n = 20	n = 46	n = 31
$\alpha+\beta$-CNBRα channels	119 ± 9	131 ± 6	1.42 ± 0.04	0.51 ± 0.04	0.75 ± 0.02
	n = 9	n = 9	n = 9	n = 13	n = 36
$\alpha+\beta$-C5 channels	18.5 ± 1.9	28.9 ± 2.1	1.47 ± 0.06	0.52 ± 0.04	1.03 ± 0.06
	n = 7	n = 7	n = 7	n = 7	n = 6
$\alpha+\beta$-M475E channels	36.9 ± 4.2	59.9 ± 4.5	1.59 ± 0.10	0.51 ± 0.02	0.87 ± 0.02
	n = 4	n = 4	n = 4	n = 4	n = 4

Data are from fits of dose-response data to Hill equations as in Fig. 3. For current amplitudes at 60 mV the peak current was measured to minimize effects of ion accumulation in the pipette (Gordon and Zagotta, 1995a). The measurements at −60 mV were usually the current amplitude at the end of the step to −60 mV.

produced by saturating cAMP almost certainly reflects a decreased ability of cAMP to induce opening once bound, suggesting that the opening of $\alpha+\beta$-CNBRα heteromultimers is less energetically favorable than the opening of either α channels or the other heteromeric channels. It is likely that the CNBR of the β subunit contains amino acid differences at positions other than 475 that affect the free energy of the opening transition.

Properties not localized to the CNBR

While the ligand-specific shift of the apparent affinities caused by the β subunit localized to the CNBR, other effects of the β subunit did not. Shallowing of the dose-response relation and desensitization were seen with all of the chimeric β/α subunits and with all three cyclic nucleotides. In addition, the gating of wild-type $\alpha+\beta$ channels was more voltage dependent than that of α channels. This is apparent both in the larger relaxation to steady state after a voltage step, and in the larger voltage dependence to the apparent affinities for cyclic nucleotide. Values of $K_{1/2}$ were ~60% greater at −60 mV than at 60 mV for $\alpha+\beta$ channels, but <10% greater for α channels (Table 1). This increased voltage dependence was seen with all of the chimeric β/α subunits and with all three cyclic nucleotides. Thus, the ligand-nonspecific effects of the β subunits, including shallowing of the dose-response relation, increased voltage dependence, rectification, and desensitization, seem to localize outside of the CNBR.

The data from $\alpha+\beta$ channels presented so far were obtained by co-injecting RNA in the oocytes at a ratio of 4:1 α:β. We wished to verify that the 4:1 co-injection ratio produces sufficient expressed β subunits to form a uniform population of heteromeric channels of their preferred stoichiometry and arrangement (Shapiro and Zagotta, 1998). Therefore, we systematically varied the α:β RNA injection ratio and examined the properties of the channels formed. Fig. 6 summarizes data from currents produced by injection of RNA for α and β subunits at ratios ranging from 2:1 to 100:1 (α:β). We focused on three parameters that distinguish α channels from $\alpha+\beta$ channels: the $K_{1/2}$ for cAMP, the Hill coefficient (n), and rectification. We found that the $K_{1/2}$ for cAMP and the Hill coefficient parameters were nearly the same for channels produced by injection ratios varying from 2:1 to 20:1 (Fig. 6, *A* and *B*). $K_{1/2}$ data for channels from a ratio of 100:1 were intermediate between those at a lower ratio and those of α channels. The rectification parameter was nearly the same at 2:1 or 4:1, somewhat higher at 20:1, and still higher at 100:1. In each case the effects of the β subunit appear to be saturating at an injection ratio of 4:1. Similar results were found for α:β-CNBRα co-injections (data not shown). These experiments suggest that an injection ratio of 4:1 is more than sufficient to produce ample β subunits, and that the channels formed

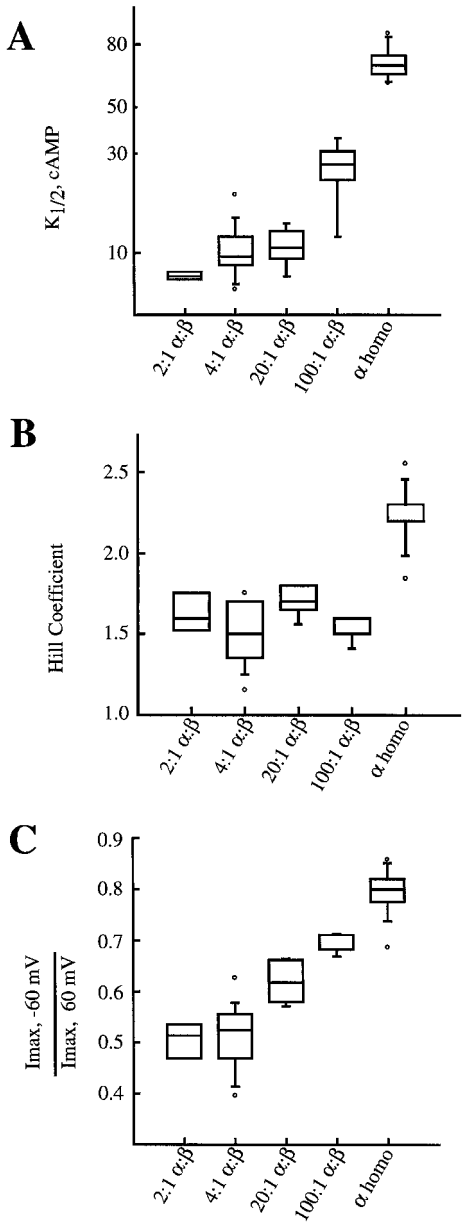

FIGURE 6 Varying the ratio of injected subunits. Data from heteromultimers from co-injections of RNA for α and wild-type β subunits at different ratios, and from α-homomultimers. Shown are box plots for the $K_{1/2}$ values (*A*), Hill coefficients (*B*), and steady-state rectification of the current (*C*), for activation of channels by cAMP. The values were taken from fits of dose-response data to a Hill equation, as in Fig. 3, from each patch. Dose-response data at 60 mV and −60 mV were separately fit to Hill equations. The I_{max} values are the steady-state currents at saturating cAMP. The horizontal line in the middle of each box marks the median of the data. The box shows the middle half of the data, between the 25th and 75th percentiles. The "whiskers" extending from some of the boxes show the data between the 5th and 95th percentiles. The circles show the extreme points in the data.

are not the result of a limiting supply of the β subunit. The saturation of the reduction in the Hill coefficient parameter at injection ratios up to 100:1 suggests that the reduced

slope is an intrinsic feature of α+β channels, and not the result of a mixture of different channel populations, although we cannot completely exclude this possibility. The intermediate behavior of channels from the 100:1 ratio could be due to a mixed population of α channels and normal α+β channels, or the result of a stoichiometry or arrangement of subunits, distinct from that preferred, caused by the scarcity of β subunits. The difference in the ratio where each of the three parameters saturated probably reflects different sensitivities of the parameters to a mixed population of channels. We predict that functional heteromeric channels have a 1:1 α:β stoichiometry (Shapiro and Zagotta, 1998), and interpret these injection-ratio data as resulting from a greater efficiency by the oocyte in expressing β subunits, relative to α subunits.

Internal Mg^{2+} block

We wondered whether replacing the CNBR of the β subunit with that of the α subunit would have any effect on channel pharmacology. We focused on the voltage-dependent pore blocker Mg^{2+} (Colamartino et al., 1991; Root and MacKinnon, 1993; Zufall and Firestein, 1993; Kleene, 1993; Dryer and Henderson, 1993; Zimmerman and Baylor, 1992; Karpen et al., 1993), and characterized the differences in internal Mg^{2+} block between α channels and α+β channels. Superimposed in Fig. 7 *A* are current-voltage curves for α channels activated by a saturating concentration of cGMP in Mg^{2+}-free solution or in the presence of various concentrations of free Mg^{2+}. Mg^{2+} block is generally greater with increasing depolarization, as expected for a

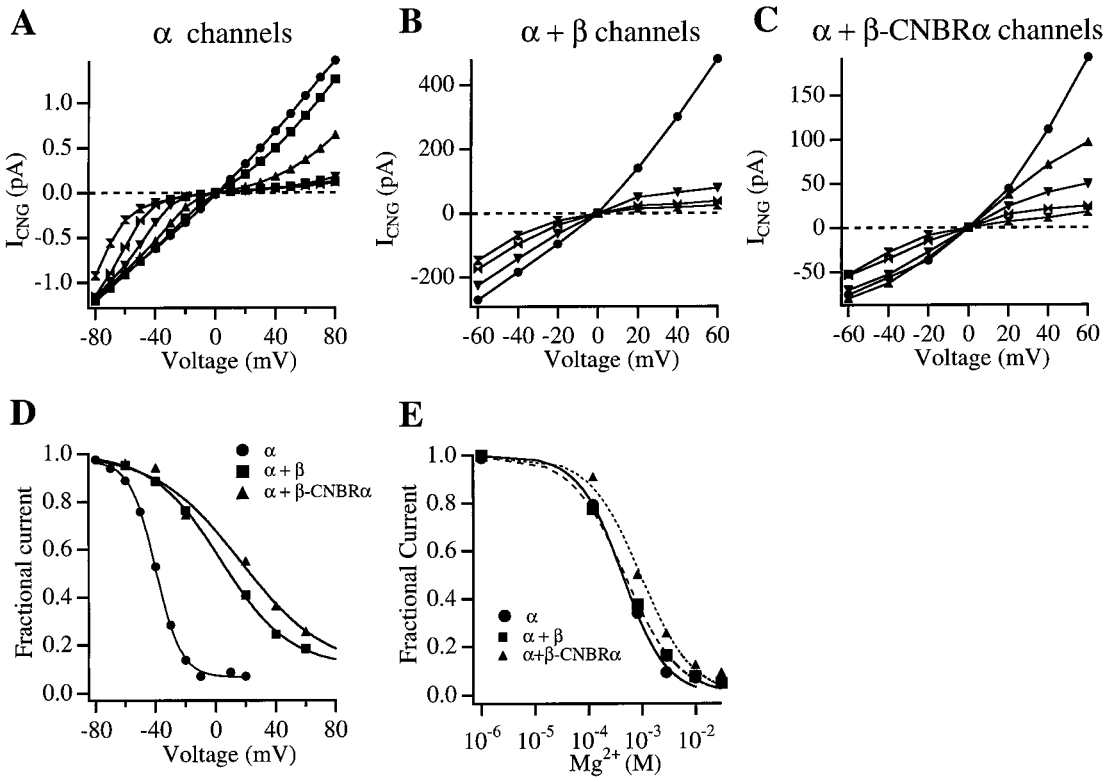

FIGURE 7 Block by internal Mg^{2+}. Current-voltage curves for a patch with α channels (*A*), α+β channels (*B*), or α+β-CNBRα channels (*C*) in the absence or presence of a range of internal Mg^{2+} concentrations. For all three panels, the Mg^{2+} concentrations are: (*circles*) 0, (*squares*) 120 μM, (*triangles*) 811 μM, (*inverted triangles*) 2.81 mM, (*bows*) 9.81 mM, (*inverted bows*) 29.8 mM. In (*A*), the data are the steady-state currents from a family of potentials from −80 mV to 80 mV at each Mg^{2+} concentration. Because of desensitization, the data in (*B*) and (*C*) were obtained by applying pseudo-ramps at each concentration, at 1/s. Each pseudo-ramp was a series of 30-ms steps progressing from −60 mV to 60 mV in 20-mV steps, and each measurement was made at the end of each step. Thus, any errors due to desensitization should be comparable to those using our usual pulse protocol (Fig. 1, *inset*). (*D*) Normalized current-voltage relations for α channels, α+β channels, and α+β-CNBRα channels at a fixed Mg^{2+} concentration of 2.81 mM. Superimposed on the data are fitted Boltzmann relations of the form $I = (I_{max} - I_s)/(1 + \exp[z\delta(V - V_{1/2})/kT]) + I_s$, where $V_{1/2}$ is the voltage at which the current is half-blocked, z is the valence of the blocker (2 for Mg^{2+}), δ is the fraction of the transmembrane electrical field sensed by the blocker, I_s is the current remaining at very positive potentials, and I_{max}, R, and T have their usual meaning. For α channels, $z\delta = 2.8e^-$ and $V_{1/2} = -56$ mV; for α+β channels, $z\delta = 1.1e^-$ and $V_{1/2} = 3$ mV; for α+β-CNBRα channels, $z\delta = 0.90e^-$ and $V_{1/2} = 17$ mV. (*E*) Normalized dose-response relations for Mg^{2+} block of the three types of channels at a fixed potential of 60 mV. Superimposed on the data are fitted Hill equation curves of the form $I = I_{max}K_{1/2}^n/(K_{1/2}^n + [Mg^{2+}]^n)$, where I is the steady-state current, $K_{1/2}$ is the concentration of Mg^{2+} that produces half-block, and n is the Hill coefficient. We constrained I_{max} to be unity. For α channels, $K_{1/2} = 425$ μM and $n = 1.06$. For α+β channels, $K_{1/2} = 469$ μM and $n = 0.88$. For α+β-CNBRα channels, $K_{1/2} = 927$ μM and $n = 0.91$.

TABLE 2 Mg^{2+} block of homo and heteromeric CNG channels

Channel	$K_{1/2}$ at 60 mV	$z\delta$ at 2.81 mM
α homomultimers	342 ± 33 μM	2.71 ± 0.15
	$n = 5$	$n = 4$
$\alpha+\beta$ heteromultimers	343 ± 50 μM	0.85 ± 0.14
	$n = 8$	$n = 7$
$\alpha+\beta$-CNBRα heteromultimers	1.53 ± 0.34 mM	1.12 ± 0.06
	$n = 4$	$n = 3$

Values of $K_{1/2}$ are from fits of Hill equation curves; values of $z\delta$ are from fits to Boltzmann equations, like those in Fig. 7.

positively charged blocker acting from the inside. At lower concentrations, the current-voltage relation is biphasic, with best block at potentials near 0 mV, but relief of block at more positive potentials, as though Mg^{2+} were weakly permeant at positive potentials. Fig. 7 *B* shows similar current-voltage curves for a patch with $\alpha+\beta$ channels. Block here is also more pronounced at more positive potentials, but the voltage dependence of the block seems much weaker. Current-voltage curves for Mg^{2+} block of $\alpha+\beta$-CNBRα channels were similar to those for $\alpha+\beta$ channels (Fig. 7 *C*), showing again voltage-dependent block weaker than that for α channels. Quantifying the voltage dependence of Mg^{2+} block of homo and heteromultimers confirmed that they were dramatically different. Fig. 7 *D* plots the block of the three types of channels as a function of voltage at a fixed concentration of 2.81 mM Mg^{2+}. The voltage dependence of block of α channels was very high, with a $z\delta$ value of $2.71e^{-} \pm 0.15$ ($n = 4$). In contrast, the voltage dependence of block of $\alpha+\beta$ channels was fairly modest, with a $z\delta$ value of $0.85e^{-} \pm 0.14$ ($n = 7$). The voltage dependence of block of $\alpha+\beta$-CNBRα channels was similarly modest, with a $z\delta$ value of $1.1e^{-} \pm 0.1$ ($n = 3$). The dose-response data for Mg^{2+} block of α channels, $\alpha+\beta$ channels, and $\alpha+\beta$-CNBRα channels at 60 mV were fit to Hill equations (Fig. 7 *E*), indicating very similar affinities at 60 mV for wild-type homo and heteromultimers, and a somewhat lower affinity for $\alpha+\beta$-CNBRα channels (Table 2). For all three channels, the slope of the Hill equation was near one, suggesting that one Mg^{2+} ion in the pore is sufficient to block the channel. Thus, the block of both types of heteromeric channels was very similar but the voltage dependencies of block of homo and heteromeric channels are strikingly different.

DISCUSSION

We find that incorporation of an olfactory β subunit (CNG5, CNCα4, OCNC2) in a heteromeric channel with the olfactory α subunit produces a large ligand-specific shift in the apparent affinities of cAMP, cGMP, and cIMP for the channel. For all three ligands, the slopes of the dose-response curves were also more shallow. Our results with cAMP and cGMP are similar to those previously reported (Bradley et al., 1994; Liman and Buck, 1994). We also show that the presence of the β subunit shifts the apparent affinity for cIMP much like for cAMP. This was somewhat surprising, given that cIMP differs from cGMP only in lacking the amino group on the 2-position of the purine ring. We localized the altered ligand discrimination to a single amino acid, M475, in the putative C-helix of the CNBR. Replacement of M475 with glutamic acid (E) was fully sufficient to transform the ligand specificity of $\alpha+\beta$-M475E heteromultimers to be like α-homomultimers. This single point mutation increased the apparent affinity for cGMP (and to a lesser extent cIMP), and decreased the apparent affinity for cAMP. The residue at position 475, then, could account for the ability of the β subunit to promote activation of olfactory channels by cAMP, their physiological ligand.

Varnum et al. (1995) have shown that an important residue for ligand discrimination in rod α channels is the acidic residue D604 in the CNBR, which is the analogous residue to M475 in the olfactory β subunit. They showed that replacement of an aspartic acid with a methionine (D604M) decreased the efficacy of cGMP (and to a lesser extent cIMP) and increased the efficacy of cAMP for rod channels (Varnum et al., 1995; Sunderman and Zagotta, 1999a). Thus, alterations in this amino acid in the C-helix produce nearly identical effects in the rod α subunit and the olfactory β subunit. Based on their results, Varnum et al. (1995) proposed a molecular mechanism to explain the cGMP specificity of the rod channels.

A similar mechanism can explain how the β subunit confers greater cAMP efficacy to the olfactory channel. Fig. 8 shows a cartoon depicting $\alpha+\beta$ channels bound by either cGMP or cAMP. For simplicity, we show only one α subunit and one β subunit; the heteromeric channels are thought to have two of each type of subunit (Shapiro and Zagotta, 1998). Illustrated are two kinds of interactions between a ligand and the C-helix of the CNBR: a strong energetically favorable interaction (shown by a yellow star), and a weak or repulsive interaction. In the α subunit, the glutamic acid at position 593 (analogous to D604 in the rod α subunit) can form hydrogen bonds with the N1 and N2 hydrogens of cGMP, making the interaction strong and very energetically favorable. A methionine at position 475 in the β subunit, however, will produce a weak interaction with cGMP. In the case of cAMP, E593 in the α subunit will be electrostatically repelled by the unshared pair of electrons at N1 of cAMP. Neutralization of this acidic residue, as in the β subunit, increases the affinity for cAMP by eliminating electrostatic repulsion. Thus, when a $\alpha+\beta$ channel is bound by cGMP, the α subunits contribute a strong interaction and the β subunits a weak one, and overall the apparent affinity for cGMP is reduced. When the channel is bound by cAMP, the β subunits contribute a strong interaction and the α subunits a weak one, and overall the apparent affinity for

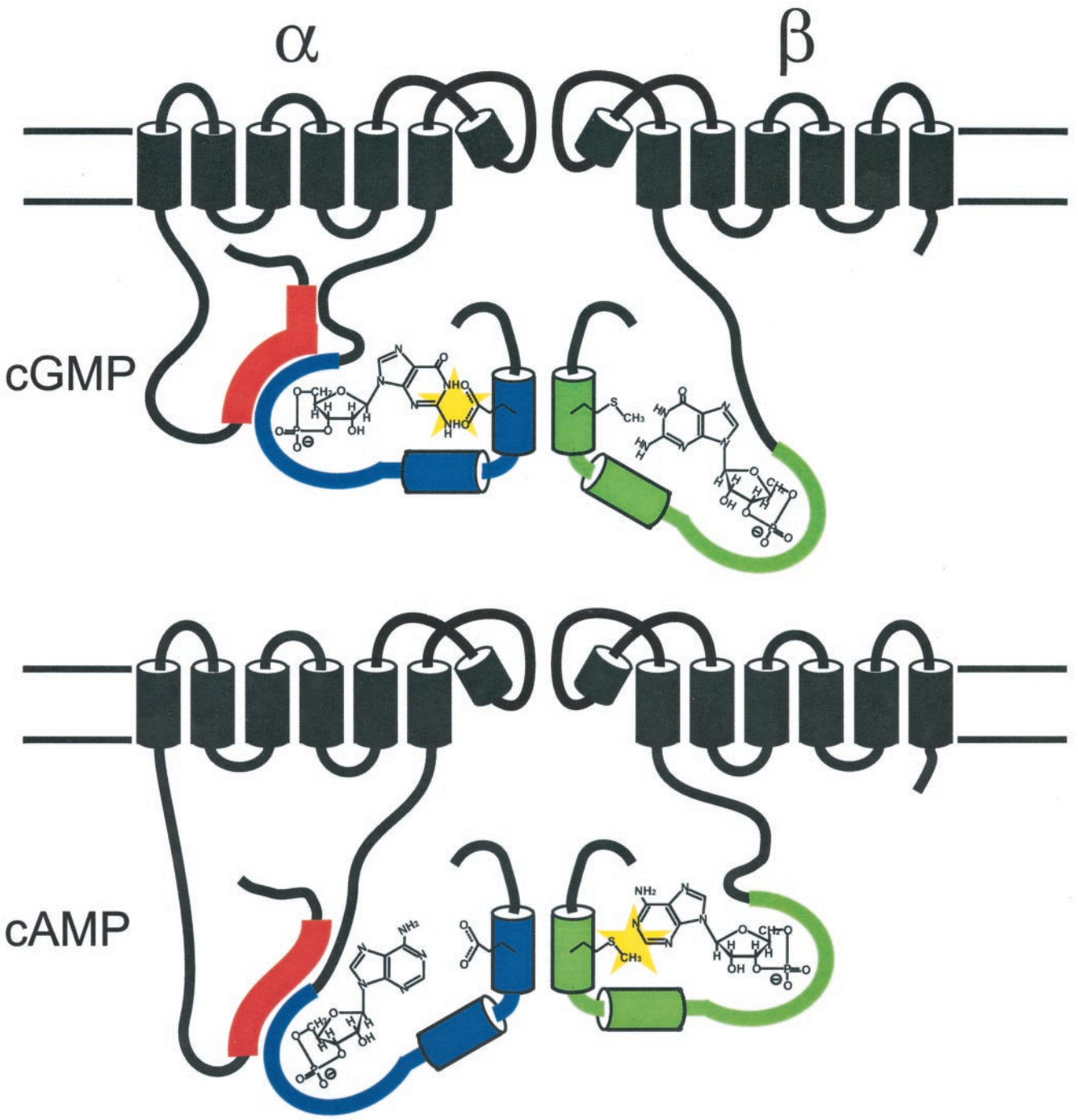

FIGURE 8 Schematic diagram showing how the β subunit alters ligand specificity in a heteromeric α+β channel. Only one α subunit and one β subunit per channel are shown for simplicity. The CNBR of the α subunits is shown in blue and of the β subunit in green. A cGMP (*top*) or cAMP (*bottom*) molecule, shown as its chemical structure, is depicted bound to the CNBR of each subunit. The purine ring of the cGMP or the cAMP is shown interacting with the C-helices (shown as cylinders). A yellow star connotes a strong interaction (see text). The red region in the amino termini of the α subunits is the autoexcitatory region of olfactory CNG channels thought to bind Ca^{2+}/calmodulin (Liu et al., 1994) and to interact with the CNBR to facilitate activation (Varnum and Zagotta, 1997). The β subunit lacks this autoexcitatory domain.

cAMP is increased. The net result is to make a channel with rather similar affinities for cGMP and cAMP.

All of our chimeric heteromultimers retained a number of the signature properties of wild-type α+β channels, indicating that these effects of the β subunit localize to a part of the channel outside of the CNBR (region depicted in black in Fig. 8). These properties include 1) a more shallow slope to the dose-response relations, 2) slow relaxation of the

current to steady state after a voltage step, 3) greater rectification at saturating cyclic nucleotide concentrations, 4) greater voltage dependence to the apparent affinity for cyclic nucleotides, 5) desensitization in the presence of maintained agonist, and 6) less voltage dependence to internal Mg^{2+} block. Unlike the effects on the apparent affinity for cyclic nucleotides, these effects were ligand independent. Thus, these signature properties of this olfactory β subunit tell us that the chimeric subunits were expressed, and their persistence in chimeric heteromultimers indicates that they do not localize to the CNBR of the β subunit.

Although the rod β subunit and the olfactory β subunit studied here have a low sequence homology (30% identity), their effects on channel properties seem similar in numerous respects. Both increase the effectiveness of cAMP as an agonist (Fodor et al., 1998; Gordon et al., 1996), both make single-channel currents more "flickery," both increase the voltage dependence of gating and rectification, both weaken divalent block, and neither forms CNG channels by itself (Chen et al., 1993; Liman and Buck, 1994; Korschen et al., 1995). Compared to α channels, expressed $\alpha+\beta$ channels behave more like native rod and olfactory channels in all of these properties (Frings et al., 1992; Nakamura and Gold, 1987; Yau and Baylor, 1989; Chen et al., 1993). The presence of an alternatively spiced variant of the rod β subunit, in addition to the olfactory β subunit cloned earlier, makes heterologously expressed olfactory channels behave even more similarly to native channels (Sautter et al., 1998; Finn et al., 1998; Bonigk et al., 1999). This rod β subunit has an asparagine at the 459 position, which is analogous to M475 in the olfactory β subunit. The D604N mutation in rod α channels also increases the relative efficacy of cAMP as an agonist (Varnum et al., 1995; Sunderman and Zagotta, 1999b). Thus, we expect the structural determinants of increased cAMP efficacy promoted by the rod β subunit to at least partly localize to this residue.

Our data indicate that Mg^{2+} is a voltage-dependent blocker of CNG channels, in accord with others (for review, see Finn et al., 1996). The partial relief of block at strongly depolarized potentials (α channels, 811 μM Mg^{2+}) is consistent with Mg^{2+} being a weakly permeant blocker, as has been observed (Colamartino et al., 1991; Frings et al., 1995; Root and MacKinnon, 1993). The voltage dependence of internal Mg^{2+} block was very different between α channels and $\alpha+\beta$ channels. In fact, the block by internal Mg^{2+} of α channels was extremely steep, with a mean $z\delta$ of $2.7e^{-}$. For a divalent blocker, this corresponds to an electrical distance 1.35 times the total membrane field. If the entire voltage dependence were due solely to occupancy of Mg^{2+} ions in the pore, this would require at least two Mg^{2+} ions at the same time. However, for a multi-ion pore, the $z\delta$ of block need not arise solely from the presence of the blocking ions themselves, but could also arise from the clearing movement of permeant ions through the pore necessary for the blocking ions to gain entry (Hille and Schwartz, 1978). Indeed, the Hill coefficient of the Mg^{2+} dose-response curve around one implies that only one Mg^{2+} ion blocks the pore, and suggests that part of the voltage dependence may arise from this mechanism. Several laboratories have shown the glutamic acid residue at position 363 in the pore of the rod α subunit is the binding site for external divalent block (Root and MacKinnon, 1993; Sesti et al., 1995; Eismann et al., 1994). At the analogous positions, the olfactory α subunit also has a glutamic acid and the β subunit has an aspartic acid. The conservative E363D mutation in rod α-homomultimers causes only a slight alteration in external Mg^{2+} block, and nonconservative mutations at this position that dramatically alter external divalent block leave internal divalent block unaffected (Root and MacKinnon, 1993; Eismann et al., 1994). Thus, we expect that differences between subunits at an as yet unidentified internal divalent blocking site can account for the large effect of the β subunit on Mg^{2+} block.

The allosteric model of Monod, Wyman, and Changeux (MWC) (Monod et al., 1965) has been used successfully to model gating of CNG channels composed of α subunits as a concerted opening transition of all the subunits (Goulding et al., 1994; Varnum and Zagotta, 1996). However, Ruiz and Karpen (1997) have suggested that CNG channels have multiple open states and that their gating should not be described by a simple MWC model. Liu et al. (1998) proposed that CNG channels gate not in a concerted fashion, but as the independent opening of two dimers of subunits. Thus, a non-concerted allosteric model may more fully describe CNG channel gating. We recently used tandem dimers to suggest that heteromeric $\alpha+\beta$ channels are composed of adjacent pairs of α subunits and β subunits (Shapiro and Zagotta, 1998). A gating mechanism involving the action of dimers of coupled subunits may reflect this subunit arrangement of functional $\alpha+\beta$ channels. A channel composed of two coupled α subunits and two coupled β subunits could provide the explanation for the decrease in the slope of the dose-response relations seen with the olfactory β subunit.

We thank Kevin Black, Heidi Utsugi, and Gay Sheridan for expert technical assistance, and Galen Flynn, Anthony Fodor, and Michael Varnum for discussions on the manuscript.

This work was supported by the Human Frontiers Science Program and by National Institutes of Health Grant 5R01-EY10329-04. W.N.Z. is an assistant investigator for the Howard Hughes Medical Institute.

REFERENCES

Anholt, R. R. 1993. Molecular neurobiology of olfaction. *Crit. Rev. Neurobiol.* 7:1–22.

Baylor, D. A., and B. Nunn. 1982. Electrical signaling in vertebrate photoreceptors. *Methods Enzymol.* 81:403–423.

Berghard, A., L. B. Buck, and E. R. Liman. 1996. Evidence for distinct signaling mechanisms in two mammalian olfactory sense organs. *Proc. Natl. Acad. Sci. USA.* 93:2365–3269.

Biel, M., X. Zong, M. Distler, E. Bosse, N. Klugbauer, M. Murakami, V. Flockerzi, and F. Hofmann. 1994. Another member of the cyclic nucleotide-gated channel family, expressed in testis, kidney, and heart. *Proc. Natl. Acad. Sci. USA.* 91:3505–3509.

Bonigk, W., J. Bradley, F. Muller, F. Sesti, I. Boekhoff, G. V. Ronnett, U. B. Kaupp, and S. Frings. 1999. The native rat olfactory cyclic nucleotide-gated channel is composed of three distinct subunits. *J. Neurosci.* 19:5332–5347.

Bradley, J., J. Li, N. Davidson, H. A. Lester, and K. Zinn. 1994. Heteromeric olfactory cyclic nucleotide-gated channels: a subunit that confers increased sensitivity to cAMP. *Proc. Natl. Acad. Sci. USA.* 91: 8890–8894.

Chen, T. Y., Y. W. Peng, R. S. Dhallan, B. Ahamed, R. R. Reed, and K. W. Yau. 1993. A new subunit of the cyclic nucleotide-gated cation channel in retinal rods. *Nature.* 362:764–767.

Colamartino, G., A. Menini, and V. Torre. 1991. Blockage and permeation of divalent cations through the cyclic GMP-activated channel from tiger salamander retinal rods. *J. Physiol. (Lond.).* 440:189–206.

Dhallan, R. S., K. W. Yau, K. A. Schrader, and R. R. Reed. 1990. Primary structure and functional expression of a cyclic nucleotide-activated channel from olfactory neurons. *Nature.* 347:184–187.

Dryer, S. E., and D. Henderson. 1993. Cyclic GMP-activated channels of the chick pineal gland: effects of divalent cations, pH, and cyclic AMP. *J. Comp. Physiol. A.* 172:271–279.

Eismann, E., F. Muller, S. H. Heinemann, and U. B. Kaupp. 1994. A single negative charge within the pore region of a cGMP-gated channel controls rectification, Ca^{2+} blockage, and ionic selectivity. *Proc. Natl. Acad. Sci. USA.* 91:1109–1113.

Finn, J. T., M. E. Grunwald, and K. W. Yau. 1996. Cyclic nucleotide gated channels: an extended family with diverse functions. *Annu. Rev. Physiol.* 58:395–426.

Finn, J. T., D. Krautwurst, J. E. Schroeder, T.-Y. Chen, R. R. Reed, and K.-W. Yau. 1998. Functional co-assembly among subunits of cyclic-nucleotide-activated, nonselective cation channels, and across species from nematode to human. *Biophys. J.* 74:1333–1345.

Fodor, A. A., K. D. Black, and W. N. Zagotta. 1998. A pore mutation that eliminates state-dependent block by tetracaine of cyclic nucleotide-gated channels. *Biophys. J.* 74:126*a*. (Abstr.).

Frings, S., J. W. Lynch, and B. Lindemann. 1992. Properties of cyclic nucleotide-gated channels mediating olfactory transduction. Activation, selectivity, and blockage. *J. Gen. Physiol.* 100:45–67.

Frings, S., R. Seifert, M. Godde, and U. B. Kaupp. 1995. Profoundly different calcium permeation and blockage determine the specific function of distinct cyclic nucleotide-gated channels. *Neuron.* 15:169–179.

Gordon, S. E., J. C. Oakley, M. D. Varnum, and W. N. Zagotta. 1996. Altered ligand specificity by protonation in the ligand binding domain of cyclic nucleotide-gated channels. *Biochemistry.* 35:3994–4001.

Gordon, S. E., and W. N. Zagotta. 1995a. A histidine residue associated with the gate of the cyclic nucleotide-activated channels in rod photoreceptors. *Neuron.* 14:177–183.

Gordon, S. E., and W. N. Zagotta. 1995b. Localization of regions affecting an allosteric transition in cyclic nucleotide-activated channels. *Neuron.* 14:857–864.

Goulding, E. H., G. R. Tibbs, and S. A. Siegelbaum. 1994. Molecular mechanism of cyclic-nucleotide-gated channel activation. *Nature.* 372: 369–374.

Hille, B., and W. Schwartz. 1978. Potassium channels as multi-ion single-file pores. *J. Gen. Physiol.* 72:409–442.

Ildefonse, M., S. Crouzy, and N. Bennett. 1992. Gating of retinal rod cation channel by different nucleotides: comparative study of unitary currents. *J. Membr. Biol.* 130:91–104.

Jan, L. Y., and Y. N. Jan. 1990. A superfamily of ion channels. *Nature.* 345:672.

Jan, L. Y., and Y. N. Jan. 1992. Tracing the roots of ion channels. *Cell.* 69:715–718.

Karpen, J. W., R. L. Brown, L. Stryer, and D. A. Baylor. 1993. Interactions between divalent cations and the gating machinery of cyclic GMP-activated channels in salamander retinal rods. *J. Gen. Physiol.* 101:1–25.

Kaupp, U. B., T. Niidome, T. Tanabe, S. Terada, W. Bonigk, W. Stuhmer, N. J. Cook, K. Kangawa, H. Matsuo, T. Hirose, T. Miyata, and S. Numa. 1989. Primary structure and functional expression from complementary DNA of the rod photoreceptor cyclic GMP-gated channel. *Nature.* 342:762–766.

Kleene, S. J. 1993. The cyclic nucleotide-activated conductance in olfactory cilia: effects of cytoplasmic Mg^{2+} and Ca^{2+}. *J. Membr. Biol.* 131:237–243.

Korschen, H. G., M. Illing, R. Selfert, F. Sesti, A. Williams, S. Gotzes, C. Colville, F. Muller, A. Dose, M. Godde, L. Molday, U. B. Kaupp, and R. S. Molday. 1995. A 240 kDa protein represents the complete β subunit of the cyclic nucleotide-gated channel from rod photoreceptor. *Neuron.* 15:627–636.

Liman, E. R., and L. B. Buck. 1994. A second subunit of the olfactory cyclic nucleotide-gated channel confers high sensitivity to cAMP. *Neuron.* 13:611–621.

Liman, E. R., J. Tytgat, and P. Hess. 1992. Subunit stoichiometry of a mammalian K^+ channel determined by construction of multimeric cDNAs. *Neuron.* 9:861–871.

Liu, M., T. Y. Chen, B. Ahamed, J. Li, and K. W. Yau. 1994. Calcium-calmodulin modulation of the olfactory cyclic nucleotide-gated cation channel. *Science.* 266:1348–1354.

Liu, D. T., G. R. Tibbs, P. Paoletti, and S. A. Siegelbaum. 1998. Constraining ligand-binding site stoichiometry suggests that a cyclic-nucleotide-gated channel is composed of two functional dimers. *Neuron.* 21:235–248.

Ludwig, J., T. Margalit, E. Eismann, D. Lancet, and U. B. Kaupp. 1990. Primary structure of cAMP-gated channel from bovine olfactory epithelium. *FEBS Lett.* 270:24–29.

McCoy, D. E., S. E. Guggino, and B. A. Stanton. 1995. The renal cGMP-gated cation channel: its molecular structure and physiological role. *Kidney Intl.* 48:1125–1133.

Monod, J., J. Wyman, and J. P. Changeux. 1965. On the nature of allosteric transitions: a plausible model. *J. Mol. Biol.* 12:88–118.

Nakamura, T., and G. H. Gold. 1987. A cyclic nucleotide-gated conductance in olfactory receptor cilia. *Nature.* 325:442–444.

Rieke, F., and E. A. Schwartz. 1994. A cGMP-gated current can control exocytosis at cone synapses. *Neuron.* 13:863–873.

Root, M. J., and R. MacKinnon. 1993. Identification of an external divalent cation-binding site in the pore of a cGMP-activated channel. *Neuron.* 11:459–466.

Ruiz, M. L., and J. W. Karpen. 1997. Single cyclic nucleotide-gated channels locked in different ligand-bound states. *Nature.* 389:389–392.

Sautter, A., X. Zong, F. Hofmann, and M. Biel. 1998. An isoform of the rod photoreceptor cyclic nucleotide-gated channel β-subunit expressed in olfactory neurons. *Proc. Natl. Acad. Sci. USA.* 95:4696–4701.

Sesti, F., U. B. Kaupp, E. Eismann, M. Nizzari, and V. Torre. 1995. The multi-ion nature of the cGMP-gated channel from vertebrate rods. *J. Physiol.* 487:17–36.

Shapiro, M. S., and W. N. Zagotta. 1998. Stoichiometry and arrangement of heteromeric olfactory cyclic nucleotide-gated ion channels. *PNAS.* 95:14546–14551.

Su, Y., W. R. G. Dostmann, F. W. Herberg, K. Durick, N.-h. Xuong, L. Ten Eyck, S. S. Taylor, and K. I. Varughese. 1995. Regulatory subunit of protein kinase A: structure of deletion mutant with cAMP binding domains. *Science.* 269:807–813.

Sunderman, E. R., and W. N. Zagotta. 1999a. Mechanism of allosteric modulation of rod cyclic nucleotide-gated channels. *J. Gen. Physiol.* 113:601–620.

Sunderman, E. R., and W. N. Zagotta. 1999b. Sequence of events underlying the allosteric transition of rod cyclic nucleotide-gated channels. *J. Gen. Physiol.* 113:621–640.

Tanaka, J. C., J. F. Eccleston, and R. E. Furman. 1989. Photoreceptor channel activation by nucleotide derivatives. *Biochemistry.* 28: 2776–2784.

Varnum, M. D., K. D. Black, and W. N. Zagotta. 1995. Molecular mechanism for ligand discrimination of cyclic nucleotide-gated channels. *Neuron.* 15:619–625.

Varnum, M. D., and W. N. Zagotta. 1996. Subunit interactions in the activation of cyclic nucleotide-gated channels. *Biophys. J.* 70: 2667–2679.

Varnum, M. D., and W. N. Zagotta. 1997. Interdomain interactions underlying activation of cyclic nucleotide-gated channels. *Science.* 278: 110–113.

Weber, I. T., and T. A. Steitz. 1987. Structure of a complex of catabolite gene activator protein and cyclic AMP refined at 2.5 Å resolution. *J. Mol. Biol.* 198:311–326.

Weyand, I., M. Godde, S. Frings, J. Weiner, F. Muller, W. Altenhofen, H. Hatt, and U. B. Kaupp. 1994. Cloning and functional expression of a cyclic-nucleotide-gated channel from mammalian sperm. *Nature.* 368: 859–863.

Yau, K. W., and D. A. Baylor. 1989. Cyclic GMP-activated conductance of retinal photoreceptor cells. *Annu. Rev. Neurosci.* 12:289–327.

Zagotta, W. N., and S. A. Siegelbaum. 1996. Structure and function of cyclic nucleotide-gated channels. *Annu. Rev. Neurosci.* 19:235–263.

Zimmerman, A. L., and D. A. Baylor. 1992. Cation interactions within the cyclic GMP-activated channel of retinal rods from the tiger salamander. *J. Physiol. (Lond).* 449:759–783.

Zufall, F., and S. Firestein. 1993. Divalent cations block the cyclic nucleotide-gated channel of olfactory receptor neurons. *J. Neurophysiol.* 69:1758–1768.

Zufall, F., S. Firestein, and G. M. Shepherd. 1994. Cyclic nucleotide-gated ion channels and sensory transduction in olfactory receptor neurons. *Annu. Rev. Biophys. Biomol. Struct.* 23:577–607.

Zufall, F., G. M. Shepherd, and C. J. Barnstable. 1997. Cyclic nucleotide gated channels as regulators of CNS development and plasticity. *Curr. Opin. Neurobiol.* 7:404–412.